ISSN 2347-3487

# ELECTROMAGNETIC ELECTRON-CYCLOTRON WAVES WITH AC FIELD IN THE MAGNETOSPHERE

R.S. Pandey[1], Rajbir Kaur[1*], S.Kumar[2] and B.S.Tomar[2]

[1]Department of Applied Physics, Amity Institute of Applied Sciences, Amity University, Noida Sector-125, India

rspandey@amity.edu

[*]Corresponding author:rkaur2@amity.edu

[2]Department of Physics, Magadh University, Bodh Gaya

## ABSTRACT

In this paper the effect of externally injected beam of cold electrons on electromagnetic electron-cyclotron (EMEC) waves in the magnetosphere has been discussed. The investigation is conducted using the methodology of characteristic solution and considering kappa distribution function in the presence of AC field. The objective of present study is to examine the variation in growth rate of EMEC waves when temperature anisotropy, magnitude of AC field and number density of energetic particles varies. It is inferred that EMEC waves grow more significantly when propagating oblique to magnetic field direction rather than parallel to magnetic field direction. Also that as the temperature anisotropy and number density of background plasma increases, growth rate of EMEC waves increases.

## Keywords:

Magnetosphere, Electron cyclotron waves, Kappa Distribution

Council for Innovative Research

Peer Review Research Publishing System

**Journal:** Journal of Advances in Physics

Vol5, No. 2

japeditor@gmail.com

www.cirjap.com

ISSN 2347-3487

## INTODUCTION

A radiation belt is an interior feature of a magnetosphere and comprises a population of energetic, electrically charged particles (electrons, protons and heavier atomic ions) durably trapped in the magnetic field of the planet. In this context the term energetic conventionally means kinetic energies E ≥ 30 keV. Each particle therein moves with constant energy and independently of all other particles along a helical path encircling a magnetic field line. The helix drifts slowly in longitude, westward for protons and other ions, and eastward for electrons. So as to generate the overall toroidal shape of the trapping region. The drift velocity is proportional to the particle's kinetic energy.

The magnetosphere properties are an essential part its gross phenomenological character. They define the external environment and reflect the internal properties of the planet. The diverse particle phenomena in the Earths magnetic field have been studied intensively, both observationally and theoretically, since Van Allen's discovery of their existence in 1958. The physical mechanisms for the creation of magnetospheric phenomena are of an electromagnetic nature. Within the solar system, the minimum condition for the existences of a planetary radiation belt is that the planet's dipole magnetic moment be sufficiently great that the flow of the solar wind is arrested before it reaches the top of the appreciable atmosphere or the surface of the planet. Otherwise, particles are lost quickly by collisions with atmospheric gas or the solid body of the planet. But even when the foregoing condition is not met, important plasma physical phenomena still occur.

Higher frequency whistler wave activity has also been observed upstream of the Earth's bow shock by plasma wave analysis. These waves possess spacecraft frame frequencies from approximately 10 to 100Hz and are generally synchronous with plasma oscillations at the electron plasma frequency [1-3] and Tokar and Gurnett [4] argued that these waves, when observed with the shock ramp result from electron beams with high thermal anisotropy and beam velocities directed towards the magnetosheath [5]. Similar high frequency whistler waves have been observed by ISEE 3 in the distant upstream plasma [6]. These waves are also coincident with electron plasma oscillations and they possibly result from streaming electrons with a solar wind, rather than a bow shock origin in accordance with the instability analysis of Gary and Feldman [7]. Orlowski et al [8] suggest that whistler waves observed in planetary foreshocks may not be the result of in situ generation, but rather these observations may simply result from propagation away from the shock.

However in the natural space environment, plasma are generally observed to possess a high-energy non-Maxwellian tail that can be modeled by a generalized Lorentzian (Kappa) distribution function that contains a spectral index κ for characterisation. The Maxwellian and kappa distributions differ substantially in the high-energy tail but differences become less significant as Kappa increases and approaches Maxwellian distribution function in the limit $\kappa \to \infty$. When the resonant particles that give rise to the growth or damping of the wave, the growth rate of a wave mode in generalized Lorentzian plasma is significantly different from that in Maxwellian plasma. Kappa distribution has also been used successfully to analyse planetary magnetospheres, spacecraft data and solar wind. [9, 10]. Hasegawa et al. [11] showed that plasma in presence of superthermal particles suffer velocity-space diffusion. That in turn leads to power law distribution at much larger velocity than the electron thermal speed. Therefore, for stability analysis of most of the space plasma should be performed using Kappa rather than Maxwellian distribution. In recent past, Pandey et al [12] have studied effect of cold plasma injection on whistler mode instability, and temporal evolution of whistler instability [13] describing cold plasma by a simple Maxwellian distribution and hot/warm background plasma in the presence of perpendicular AC field by a generalized distribution function reducible to bi- Maxwellian and loss-cone in the magnetosphere of Uranus.

## MATHEMATICAL FORMULATION:

A spatially homogeneous anisotropic, collisionless plasma subjected to external magnetic field $\mathbf{B_o} = B_o \hat{\mathbf{e}}_z$ and an electric field $\mathbf{E_o} = E_o \sin(\upsilon t)\hat{\mathbf{e}}_x$ has been considered to get dispersion relation. In this case, linearized Vlasov-Maxwell equations, obtained after neglecting higher order terms and separating the equilibrium and non-equilibrium parts, following the technique of Pandey [14] and Misra and Pandey [12], are given as below:

$$\mathbf{v}.\left(\frac{\partial f_{so}}{\partial \mathbf{r}}\right) + \frac{e_s}{m_s}\left[E_o \sin(\upsilon t) + (\mathbf{v}\times\mathbf{B_o})\right]\left(\frac{\partial f_{so}}{\partial \mathbf{v}}\right) = 0 \quad (1)$$

$$\frac{\partial f_{s1}}{\partial t} + \mathbf{v}.\left(\frac{\partial f_{s1}}{\partial \mathbf{r}}\right) + (F/m_s)\frac{\partial f_{s1}}{\partial \mathbf{v}} = S(\mathbf{r},\mathbf{v},t) \quad (2)$$

Where force is given as $F = m\dfrac{dv}{dt}$

$$\mathbf{F} = e_s\left[E_o \sin(\upsilon t) + (\mathbf{v}\times\mathbf{B_o})\right] \quad (3)$$

The particle trajectories are obtained by solving equation of motion defined in equation (3) and S(r,v,t) is defined as:

$$S(\mathbf{r},\mathbf{v},t) = (e/m_s)\left[E_1 + (\mathbf{v}\times\mathbf{B_1})\right]\left(\frac{\partial f_{so}}{\partial \mathbf{v}}\right) \quad (4)$$

where s denotes species and $E_1$, $B_1$ and $f_{s1}$ are perturbed quantities and are assumed to have harmonic dependence in $E_1$, $B_1$ and $f_{s1}$=exp i(**k**.**r** − ωt).

The method of characteristic solution is used to determine the perturbed distribution function, fs1, which is obtained from Eq. (2) by

$$f_{s1}(\mathbf{r},\mathbf{v},t)=\int_0^{\infty} s\{\mathbf{r_o}(\mathbf{r},\mathbf{v},t'),\mathbf{v_o}(\mathbf{r},\mathbf{v},t'),t-t'\}dt' \tag{5}$$

The phase space coordinate system has been transformed from $(\mathbf{r},\mathbf{v},t)$ to $(\mathbf{r_o},\mathbf{v_o},t-t')$. The particle trajectories which are obtained by solving eq. (3) for the given external field and wave propagation, $\mathbf{k}=\lfloor \mathbf{k}_{\perp}\hat{e}_x,0,\mathbf{k}_{||}\hat{e}_z \rfloor$ are:

$$\mathbf{x_o}=\mathbf{x}+\left(\frac{\mathbf{v_y}}{\omega_{cs}}\right)+\left(\frac{1}{\omega_{cs}}\right)\left[\mathbf{v_x}\sin\omega_{cs}t'-\mathbf{v_y}\cos\omega_{cs}t'\right]+\left(\frac{\Gamma_x}{\omega_{cs}}\right)\left[\frac{\omega_{cs}\sin\upsilon t'-\upsilon\sin\omega_{cs}t'}{\omega_{cs}^2-\upsilon^2}\right] \tag{6a}$$

$$\mathbf{y_o}=\mathbf{y}+\left(\frac{\mathbf{v_x}}{\omega_{cs}}\right)-\left(\frac{1}{\omega_{cs}}\right)\left[\mathbf{v_x}\cos\omega_{cs}t'-\mathbf{v_y}\sin\omega_{cs}t'\right]-\left(\frac{\Gamma_x}{\omega_{cs}}\right)\left[1+\frac{\upsilon^2\cos\omega_{cs}t'-\omega_{cs}^2\cos\upsilon t'}{\omega_{cs}^2-\upsilon^2}\right] \tag{6b}$$

$$\mathbf{z_o}=\mathbf{z}-\mathbf{v_z}t' \tag{6c}$$

And the velocities are

$$\mathbf{v_{xo}}=\mathbf{v_x}\cos\omega_{cs}t'-\mathbf{v_y}\sin\omega_{cs}t'+\left\{\frac{\upsilon\Gamma_x(\cos\upsilon t'-\cos\omega_{cs}t')}{\omega_{cs}^2-\upsilon^2}\right\} \tag{7a}$$

$$\mathbf{v_{yo}}=\mathbf{v_x}\sin\omega_{cs}t'+\mathbf{v_y}\cos\omega_{cs}t'-\left\{\frac{\Gamma_x}{(\omega_{cs}\sin\upsilon t'-\upsilon\sin\omega_{cs}t')}\omega_{cs}^2-\upsilon^2\right\} \tag{7b}$$

$$\mathbf{v_{zo}}=\mathbf{v_z} \tag{7c}$$

Where $\omega_{cs}=\frac{e_sB_o}{m_s}$ =cyclotron frequency of species s

$\Gamma_x=\frac{e_sE_o}{m_s}$ = a.c electric field varying as $E=E_{ox}\sin(\upsilon t)$

$\upsilon$ = angular a.c frequency

After some algebraic simplifications and integration, the perturbed distribution function is given as:

$$f_{s1}(\mathbf{r},\mathbf{v},t)=-\frac{e_s}{m_s\omega}\sum_{m,n,p,q}^{\infty}\frac{J_p(\lambda_2)J_m(\lambda_1)J_q(\lambda_3)e^{i(k.r-\omega t)}}{\{\omega-\mathbf{k}_{||}\mathbf{v}_{||}-(n+q)\omega_{cs}+p\upsilon\}}\left[E_{1x}J_nJ_p\left\{\left(\frac{n}{\lambda_1}\right)U^*+D_1\left(\frac{p}{\lambda_2}\right)\right\}-iE_{1y}\{J'_nJ_pC_1+J_nJ'_pD_2\}+E_{1x}J_nJ_pW^*\right]$$

Where $e^{i(\sin\theta)\lambda}=\sum_{k=-\infty}^{\infty}J_k(\lambda)e^{ik\theta}$ is the Bessel identity. It has been used as an argument of the following functions:

$$\lambda_1=\frac{\mathbf{k}_{\perp}\mathbf{v}_{\perp}}{\omega_{cs}},\qquad \lambda_2=\frac{\mathbf{k}_{\perp}\Gamma_x\upsilon}{\omega_{cs}^2-\upsilon^2},\qquad \lambda_3=\frac{\mathbf{k}_{\perp}\Gamma_x\upsilon}{\omega_{cs}^2-\upsilon^2} \tag{8a}$$

$$C_1=\frac{1}{\mathbf{v}_{\perp}}\left(\frac{\delta f_o}{\delta\mathbf{v}_{\perp}}\right)(\omega-\mathbf{k}_{||}\mathbf{v}_{||})+\left(\frac{\delta f_o}{\delta\mathbf{v}_{||}}\right)\mathbf{k}_{||} \tag{8b}$$

$$U^*=C_1\left[\mathbf{v}_{\perp}-\left(\frac{\upsilon\Gamma_x}{\omega_{cs}^2-\upsilon^2}\right)\right] \tag{8c}$$

$$W^*=\left[\left(n\omega_{cs}\frac{\mathbf{v}_{||}}{\mathbf{v}_{\perp}}\right)\left(\frac{\delta f_o}{\delta\mathbf{v}_{\perp}}\right)-n\omega_{cs}\left(\frac{\delta f_o}{\delta\mathbf{v}_{\perp}}\right)\right]+\left[1+\left\{\frac{\mathbf{k}_{\perp}\Gamma_x\upsilon}{\omega_{cs}^2-\upsilon^2}\right\}\left\{\frac{p}{\lambda_2}-\frac{n}{\lambda_1}\right\}\right] \tag{8d}$$

$$D_1 = C_1\left(\frac{\upsilon\Gamma_x}{\omega_{cs}^2 - \upsilon^2}\right), \qquad D_2 = C_1\left(\frac{\omega_{cs}\Gamma_x}{\omega_{cs}^2 - \upsilon^2}\right)$$

$$J_n' = \frac{dJ_n(\lambda_1)}{d\lambda_1}, \qquad J_p' = \frac{dJ_p(\lambda_2)}{d\lambda_2} \tag{8f}$$

The conductivity tensor is written as: $\| \boldsymbol{\sigma} \| = -\sum\left(\frac{e_s}{m_s\omega}\right)\sum_{m,n,p,q=-\infty}^{\infty}\int d^3\mathbf{v}\left[\frac{J_q(\lambda_3)S_{ij}}{\omega - \mathbf{k}_{||}\mathbf{v}_{||} - (n+q)\omega_{cs} + p\upsilon}\right]$ (9)

$$\| \mathbf{S} \| = \begin{vmatrix} \mathbf{v}_\perp J_n^2 J_p\left(\frac{n}{\lambda_1}\right)A & i\mathbf{v}_\perp J_n B & \mathbf{v}_\perp J_n^2 J_p\left(\frac{n}{\lambda_1}\right)W^* \\ \mathbf{v}_\perp J_n' J_n J_p A & \mathbf{v}_\perp J_n' B & i\mathbf{v}_\perp J_n' J_n J_p W^* \\ \mathbf{v}_{||} J_n^2 J_p A & \mathbf{v}_{||} J_n B & \mathbf{v}_{||} J_n^2 J_p W^* \end{vmatrix} \tag{10}$$

$$A = \left(\frac{n}{\lambda_1}\right)U^* + \left(\frac{p}{\lambda_1}\right)D_1 \qquad B = J_n' J_p C_1 + J_n' J_n D_2 \tag{11}$$

From $J = \| \boldsymbol{\sigma} \| E_1$ and two Maxwell's curl equations for the perturbed quantities, the wave equations can be written as:

$$\left[\mathbf{k}^2 - \mathbf{k}.\mathbf{k} - \left(\omega^2/c^2\right) \in (\mathbf{k},\omega)\right]E_1 = 0 \tag{12}$$

Where $\| \in (\mathbf{k},\omega) \| = 1 - (4\pi/i\omega)\| \boldsymbol{\sigma}(\mathbf{k},\omega) \|$ = dielectric tensor (13)

$$\in_{ij}(k,\omega) = 1 + \sum_s \frac{4e_s^2\pi}{m_s\omega^2}\sum_n\sum_p J_p(\lambda_2)J_q(\lambda_3)\int \frac{d^3vS_{ij}}{\omega - k_{||}v_{||} - (n+q)\omega_{cs} + p\upsilon} \tag{14}$$

The generalized dielectric tensor may be written as:

$$\begin{vmatrix} N^2\cos^2\theta_1 + \varepsilon_{11} & \varepsilon_{12} & N^2\cos\theta_1\sin\theta_1 + \varepsilon_{13} \\ \varepsilon_{21} & N^2 + \varepsilon_{22} & \varepsilon_{23} \\ N^2\cos\theta_1\sin\theta_1 + \varepsilon_{31} & \varepsilon_{32} & N^2\sin^2\theta_1 + \varepsilon_{33} \end{vmatrix} \tag{15}$$

After using the limits in above tensor $\mathbf{k}_\perp = k\sin\theta_1 \to 0$ and $\mathbf{k}_{||} = k\cos\theta_1$, the generalized dielectric tensor becomes simplified tensor:

$$\begin{vmatrix} -N^2 + \varepsilon_{11} & \varepsilon_{12} & 0 \\ -\varepsilon_{21} & -N^2 + \varepsilon_{22} & 0 \\ 0 & 0 & \varepsilon_{33} \end{vmatrix} \tag{16}$$

For EMEC waves, it is rewritten in more convenient form:

$$-N^4 - 2\varepsilon_{11}N^2 + \varepsilon_{11}^2 + \varepsilon_{12}^2 = 0 \tag{17}$$

Neglecting the higher order terms of N, the relation becomes:

$$\varepsilon_{11} \pm \varepsilon_{12} = N^2 \tag{18}$$

Where N is index of refraction.

The unperturbed Lorentzian-Kappa distribution function is:

$$F_{ok} = \frac{n_o}{\pi^{3/2}\theta_1^2\boldsymbol{\theta}_{||}k^{3/2}}\frac{\Gamma(k+1)}{\Gamma(k+1/2)}\left[1 + \frac{\mathbf{v}_{||}^2}{k\boldsymbol{\theta}_{||}^2} + \frac{\mathbf{v}_\perp^2}{k\boldsymbol{\theta}_\perp^2}\right]^{-(k+1)} \tag{19}$$

And associated parallel and perpendicular effective thermal speeds are

$$\boldsymbol{\theta}_{\|}=\left[\frac{2k-3}{k}\right]^{1/2}\left(\frac{T_{\|}}{m_s}\right)^{1/2}, \qquad \boldsymbol{\theta}_{\perp}=\left[\frac{2k-3}{k}\right]^{1/2}\left(\frac{T_{\perp}}{m_s}\right)^{1/2}$$

Applying the approximation in electron-cyclotron range of frequencies. In this case, ion temperature are assumed $T_{is}=T_{i\|}=T_i$ and assumed to be magnetized with $|\omega_r+i\gamma|<<\omega_{cs}$ while electrons are assumed to have $T_{\perp e}>T_{\|e}$ and $|k_{\|}\alpha_{\|}|<<|\omega_r\pm\omega_{cs}+i.\gamma|$ for background plasma. Therefore Equation (19) becomes the following, as a sum of background and injected cold beam plasma:

$$D(k,\omega_r+i\gamma)=1-\frac{k^2c^2}{\omega_r+i\gamma}+\sum\frac{J_p(\lambda_2)J_q(\lambda_3)}{\alpha_{\perp s}^2}\left[\left\{\frac{\omega_i^2}{\omega_{ce}^2}-\frac{\omega_{pi}^2}{(\omega_r+i\gamma)\pm\omega_{ce}}\right\}\left\{X_1 i\frac{\omega_{pi}^2}{(\omega_r+i\gamma)}\right\}\frac{\omega_r+i\gamma}{k_{\|}\theta_{\|e}}\left(\frac{k-1}{k}\right)^{1/2}\right]\times$$

$$\left[\left(\frac{k-1}{k-3/2}\right)Z_{k-1}\left(\left(\frac{k-1}{k}\right)1/2\xi_e\right)A_T\left\{1+\xi_e\left(\left(\frac{k-1}{k}\right)^{1/2}\left(\frac{k-1}{k-3/2}\right)Z_{k-1}^{*}\left(\frac{k-1}{k}\right)^{1/2}\xi_e\right)\right\}\right]-\frac{\omega}{\omega\pm\omega_c}\frac{\omega_{pc}^2}{\omega_{pw}^2} \qquad (20)$$

Where $X_{1i}=\theta_{\perp i}^2-\frac{\upsilon\Gamma_{xi}}{\omega_{ci}^2-\upsilon^2}\frac{\theta_{\perp i}}{2}\sqrt{\pi}$

$$X_{1e}=\theta_{\perp e}^2-\frac{\upsilon\Gamma_{xe}}{\omega_{ce}^2-\upsilon^2}\frac{\theta_{\perp e}}{2}\sqrt{\pi}$$

$$A_T=\frac{\theta_{\perp e}^2}{\theta_{\|e}^2}-1$$

$Z(\xi)=$ Plasma Dispersion Function

Applying condition $\frac{k^2c^2}{\omega^2}>>1+\frac{\omega_{pi}^2}{\omega_{ci}^2}$ with p=1, n=1 and q=0 we can get the growth rate and real frequency using $K_3=1-X_3+X_4$, $K_4=\frac{X_3}{1-X_3+X_4}$, $\tilde{\mathbf{k}}=\frac{\mathbf{k}_{\|}\boldsymbol{\alpha}_{\|}}{\omega_{cs}}$, $\beta=\frac{K_B T_{\|}\mu_o n_o}{B_o^2}$ $\Gamma_{xs}=\frac{eE_o}{m_s}$ $X_4=\frac{-\upsilon}{\omega_{ce}}$

$$\delta=1+\frac{n_c}{n_w}(1+X_4)$$

$$\frac{\gamma}{\omega_{ce}}=\frac{\frac{\sqrt{\pi}}{\tilde{\mathbf{k}}}\left(\frac{(k-1)!k^{k-1/2}}{(k-3/2)!}\right)(A_T-K_4)K_3^3\left\{-\left(\frac{k^3}{\tilde{\mathbf{k}}}\right)\right\}^{-2k}}{1+X_4+\frac{k}{k-3/2}\left[\frac{(1+X_4)\tilde{\mathbf{k}}^2}{2K_3^2}+\frac{\tilde{\mathbf{k}}^2}{K_3}(A_T-K_4)\right]-\frac{X_{1e}}{X_{1i}}K_3^2+\frac{(\delta-1)K_3^2}{(1-X_3)^2(1+X_4)}} \qquad (21)$$

$$X_3=\frac{\omega_r}{\omega_{ce}}=\frac{\tilde{\mathbf{k}}^2}{\delta\beta}\left[\frac{X_{1e}(1+X_4)}{X_{1e}-X_{1i}(1+X_4)}+\frac{A_T\beta X_{1e}}{2(1+X_4)(X_{1e}-X_{1i}(1+X_4))}\right] \qquad (22)$$

When EMEC waves propagate oblique to magnetic field direction, referring to equation no. (15), the reduced dielectric tensor in equation (18) becomes:

$$\varepsilon_{11}\pm\varepsilon_{12}=N^2\cos^2\theta \qquad (23)$$

Using equation (23) and equation (19), following the similar approach, the expression of growth rate and real frequency becomes:

$$\frac{\gamma}{\omega_{ce}} = \frac{\frac{\sqrt{\pi}}{\tilde{\mathbf{k}}\cos\theta}\left(\frac{(k-1)!\,k^{k-1/2}}{(k-3/2)!}\right)(A_T - K_4)K_3^3\left\{-\left(\frac{k^3}{\tilde{\mathbf{k}}\cos\theta}\right)\right\}^{-2k}}{1+X_4+\frac{k\cos^2\theta}{k-3/2}\left[\frac{(1+X_4)\tilde{\mathbf{k}}^2}{2K_3^2}+\frac{\tilde{\mathbf{k}}^2}{K_3}(A_T-K_4)\right]-\frac{X_{1e}}{X_{1i}}K_3^2+\frac{(\delta-1)K_3^2}{(1-X_3)^2(1+X_4)}} \quad (24)$$

$$X_3 = \frac{\omega_r}{\omega_{ce}} = \frac{\tilde{\mathbf{k}}^2\cos^2\theta}{\delta\beta}\left[\frac{X_{1e}(1+X_4)}{X_{1e}-X_{1i}(1+X_4)}+\frac{A_T\beta X_{1e}}{2(1+X_4)(X_{1e}-X_{1i}(1+X_4))}\right] \quad (25)$$

## DISCUSSION:

## Plasma Parameters:

To study the variation of dimensionless growth rate of electromagnetic electron-cyclotron waves consisting of kappa distribution function, following plasma parameters have been considered $B_0$ = 1x10$^{-7}$T, $E_o$ = 4 mV/m, $k_B T_{\|i}$=100eV, $k_B T_{\|e}$=5KeV, $T_\perp/T_\|$ = 1.25, 1.5, 1.75, $\upsilon$ = 2KHz, 3KHz, 4KHz and $n_c/n_w$ = 10,15,20,30. When oblique propagation of EMEC waves is studied, the angle of propagation is varied too. According to this choice of plasma parameters, the discussion of the results is given.

## For Parallel Propagation

**Figure 1** shows the **v**ariation of growth rate with respect to $\tilde{k}$ for various values of temperature anisotropy $A_T$ of background plasma and other fixed parameters as listed in figure caption. Since $A_T = [(T_\perp/T_\|) - 1]$, $A_T$ becomes 0.25, 0.50 and 0.75. For $T_\perp/T_\|$ =1.25, 1.5 and 1.75, the growth rate is 0.00516, 0.0075 and 0.0112 respectively. The maxima changes from $\tilde{k}$ =0.20 to $\tilde{k}$ =0.21 and $\tilde{k}$ =0.22. As the value of $A_T$ increases, growth rate increases. In this graph the growth rate increases with increase of temperature anisotropy and maxima is shifted towards the higher k values. It is clear from the figure that the temperature anisotropy is the main source of energy to drive the excitation of the wave. In **figure 2** variation of dimensionless growth rate with respect to $\tilde{k}$ for various values of AC frequencies is shown with other fixed parameters as mentioned in figure caption. The growth rate is 0.00516, 0.0060 and 0.0067 for $\upsilon$ = 2 KHz, 3 KHz and 4 KHz at $\tilde{k}$ =0.20, $\tilde{k}$ =0.19 and $\tilde{k}$ =0.18 respectively. It is seen that growth rate increases with increase in AC frequency but maxima shifts to lower value of wave number. **Figure 3** shows the variation of growth rate with $\tilde{k}$ for various values of ratio of number density of cold electrons to hot electrons. The number density of hot background plasma is assumed variable as 5x10$^6$m$^{-3}$, 2.5x10$^6$m$^{-3}$ and 1.6x10$^6$ m$^{-3}$, thus giving $n_c/n_w$ as 10, 20 and 30 (approximately). The growth rate is 0.00516 for $n_c/n_w$ =10 at $\tilde{k}$ =0.20, the growth rate is 0.0071 when $n_c/n_w$ =20 at $\tilde{k}$ =0.28 and growth rate is $\gamma/\omega_c$ =0.0087 for $n_c/n_w$ =30 at $\tilde{k}$ =0.34. This shows that as the number density of hot electrons decreases, that is, as the ratio of $n_c/n_w$ increases from 10 to 30, growth rate increases. The increase in bandwidth and significant shift in $\tilde{k}$ value is also seen in graph from 0.20 to 0.34 for kappa distribution index κ= 2. Results can be compared with Pandey et al. [15]

Lorentzian/Kappa plasma series expansion brings change in thermal velocity (perpendicular), affecting terms of temperature anisotropy. Temperature anisotropy being the primary source of instability gets further modified by Kappa distribution function, giving rise to further increase in growth rate. The theory of kappa distribution also explains that suprathermal electron in Kappa distribution modifies the intensity and Doppler frequency of electron plasma lines. (Reference). The inclusion of temperature anisotropy in Lorentzian (Kappa) plasma can explain the observed higher frequencies spectrum of whistler waves [16,17].

## For Oblique Propagation

**Figure 4** shows the **v**ariation of dimensionless growth rate with respect to $\tilde{k}$ for various values of temperature anisotropy, $T_\perp/T_\|$ -1, and other fixed parameters as listed in figure caption. The growth rate is 0.00513 for $T_\perp/T_\|$ =1.25 at $\tilde{k}$ =0.20, the growth rate is 0.0074 when $T_\perp/T_\|$ =1.5 at $\tilde{k}$ =0.22 and growth rate is $\gamma/\omega_c$ =0.0108 for $T_\perp/T_\|$ =1.75 at $\tilde{k}$ =0.24. As the temperature anisotropy in the background plasma increases the growth rate of obliquely propagating EMEC waves, increases. Although the difference in increase of growth rate is less as compared to figure 1 of parallel propagation but the bandwidth increases in case of oblique propagation. **Figure 5** shows the variation of dimensionless growth rate with respect to $\tilde{k}$ for various values of magnitude of AC frequencies at other plasma parameters being fixed and listed in the figure caption. The figure shows that for different values of AC frequency the peak value of growth rate appears at wave number $\tilde{k}$ =0.20. For $\upsilon$ = 2 KHz, 3 KHz and 4KHz, growth rate is $\gamma/\omega_c$ = 0.00513, 0.060, 0.0066 respectively. It is seen that growth rate increases with increasing value of $\upsilon$. The growth rate increases with increase in value of a.c. frequency due to negative exponential of Landau damping. Also maxima shifts to lower values of $\tilde{k}$ showing that the a.c. frequency

modifies resonance frequency. The perpendicular electric field contributes significantly to the emission of VLF signals and explains the low frequency side of the spectrum. The modification of perpendicular velocity contributes to energy exchange between electrons, components of the wave electric field and the impressed AC field. Thus leading to growth or the damping of cyclotron waves. **Figure 6** shows the variation of dimensionless growth rate with respect to $\tilde{k}$ for various values of ratio of number density of cold electrons to hot electrons. The figure explains that for $n_c/n_w$ = 10, 20 and 30, peak values occur at $\tilde{k}$ =0.20, 0.28 and 0.34 respectively. For different ratio of number density the growth rate varies slightly ie. $\gamma/\omega_c$ = 0.00513 for $n_c/n_w$ = 10, $\gamma/\omega_c$ = 0.0070 for $n_c/n_w$ = 20 and $\gamma/\omega_c$ = 0.0087 for $n_c/n_w$ = 30. Second harmonic generation for higher ratio of cold to hot electrons number density can be seen in this figure. Also the bandwidth increases significantly when injection of more cold electrons is considered. **Figure 7** shows the variation of relativistic dimensionless growth rate with respect to $\tilde{k}$ for various angles of propagation $\theta$, at other plasma parameters being fixed and stated in figure caption. At $\tilde{k}$ = 0.20, $\gamma/\omega_c$ = 0.00513 for $\theta$=10°, at $\tilde{k}$ = 0.22, $\gamma/\omega_c$ = 0.0050 for $\theta$=20° and at $\tilde{k}$ = 0.24, $\gamma/\omega_c$ = 0.0049 for $\theta$=30°. It is seen that growth rate decreases with increasing value of ratio of $\theta$. This implies that growth rate increases more when waves propagate parallel to magnetic field direction that in case of oblique propagation.
Study can be compared with Pandey et al. [18]

**Case I : Parallel Propagation**

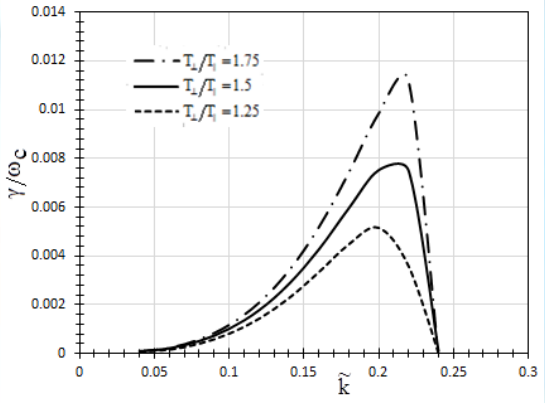


**Fig 1. Variation of Growth Rate and Real Frequency with respect to $\tilde{k}$ for various values of $T_\perp/T_{||}$ at $n_o$=4x10$^4$m$^{-3}$, $\upsilon$=2Hz and other fixed plasma parameters.**

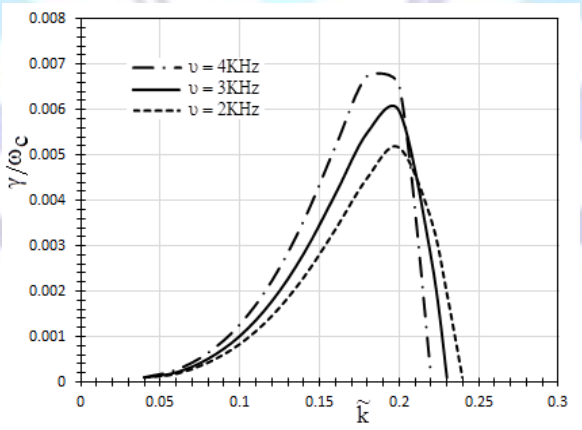


**Fig 2. Variation of Growth Rate and Real Frequency with respect to $\tilde{k}$ for various values of AC frequency $\upsilon$, at $T_\perp/T_{||}$ =1.25, $n_o$=4x10$^4$m$^{-3}$ and other fixed plasma parameters.**

ISSN 2347-3487

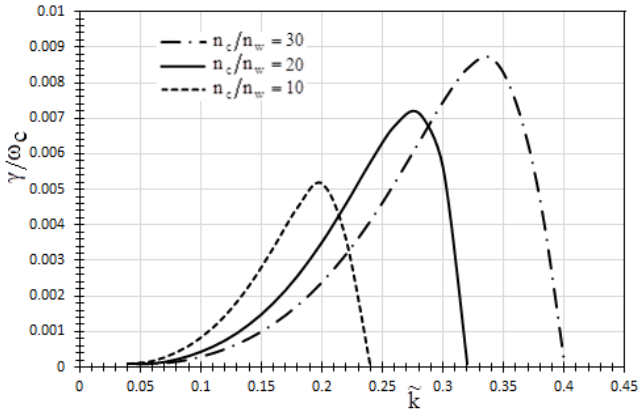


**Fig 3. Variation of Growth Rate and Real Frequency with respect to $\tilde{k}$ for various values of $n_c/n_w$ at $T_\perp/T_{ll}$ =1.25, $n_o$=4x10$^4$m$^{-3}$ and other fixed plasma parameters.**

## Case II : Oblique Propagation

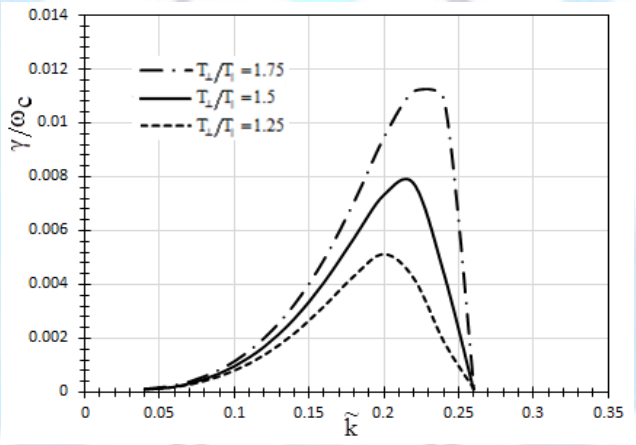


**Fig 4. Variation of Growth Rate and Real Frequency with respect to $\tilde{k}$ for various values of $T_\perp/T_{ll}$ at $n_o$=4x10$^4$m$^{-3}$, $\upsilon$=2Hz, $\theta$=10$^o$ and other fixed plasma parameters.**

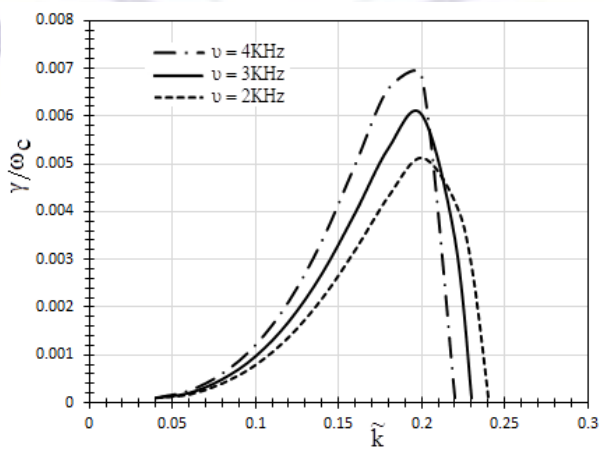


**Fig 5. Variation of Growth Rate and Real Frequency with respect to $\tilde{k}$ for various values of AC frequency, $\upsilon$, at $T_\perp/T_{ll}$ =1.25, $n_o$=4x10$^4$m$^{-3}$, $\theta$=10$^o$ and other fixed plasma parameters**

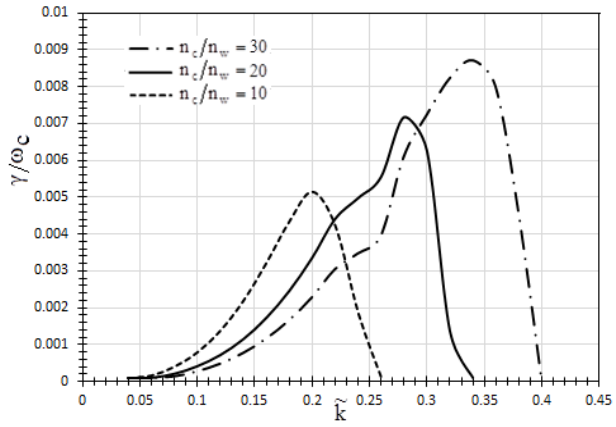


**Fig 6. Variation of Growth Rate and Real Frequency with respect to $\tilde{k}$ for various values of $n_c/n_w$ at $T_\perp/T_{ll}$ =1.25, $n_o$=4x10$^4$m$^{-3}$ and other fixed plasma parameters.**

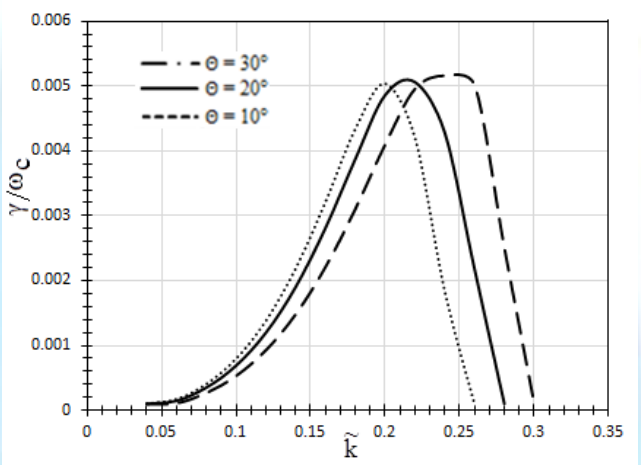


**Fig 7. Variation of Growth Rate and Real Frequency with respect to $\tilde{k}$ for various values of oblique angle, $\theta$, at $T_\perp/T_{ll}$ =1.25, $n_o$=4x10$^4$m$^{-3}$, $\upsilon$=2Hz and other fixed plasma parameters.**

## REFERENCES


[1] Anderson, R. R., Parks, G.K., Eastman, T.E., Gurnett, D.A. and Frank, L.A., Plasma waves associated with energetic particles streaming into the solar wind from the Earth's bow shock, J. Geophys. Res., Vol. 86, 4493

[2] Greenstadt, E. W., Fredericks, R.W., Russel, C.T., Scarf, F.L., Anderson, R.R. and Gurnett, D.A., 1981, Whistler mode wave propagation in the solar wind near the bow shock, J. Geophys,Res., Vol. 86, 4511

[3] Toker, R. L., Gurnett, D.A. and Feldman, W.C.,1984, Whistler mode turbulence generated by electron beams in Earth's bow shock, J. Geophys. Res., Vol. 89, 105

[4] Tokar, R. L. and Gurnett, D.A., 1985, The propagation and growth of whistler mode wave generated by electron beam in Earth's bow shock, J. Geophys. Res., Vol. 90, 105

[5] Feldman, W. C., Anderson, R.C., Bame, S.J., Gary, S.P., Gosling, J.T., McComas, D.J., Thomson, M.F., Paschmann, G. and Hoppe, M.M., 1983, Electron velocity distributions near the Earth's bow shock, J. Geophys. Res., Vol. 88, 96

[6] Kennel, C. F., Scarf, F.L., Coroniti, F.V., Fredericks, R.W., Gurnnett, D.A. and Smith, E.J., 1980, Correlated whistler and electron plasma oscillation burst detected on ISEE 3, Geophys. Res. Lett., Vol. 7, 129

[7] Gary, S. P. and Feldman, W.C, 1977, Solar wind heat flux regulation by the whistler instability, J. Geophys Res., Vol. 82, 1087

[8] Orlowski, D. S., Crawford, G.K. and Russel, C.T., 1990, Upstream waves at mercury, venus and earth, comparisons of the properties of one Hertz waves, Geophys Res. Lett., Vol. 17, 2293

[9] Abraham-Shrauner, B., Asbridge, J.R., Bame, S.J. and Feldman W.C., 1979, Proton-driven electromagnetic instabilities in high-speed solar wind streams, J. Geophys. Res., Vol. 84, 553

[10] Mace, R. L.,1998, Whistler instability enhanced by superathermal electrons within the Earth's foreshock, J. Geophys. Res., Vol. 103, 14643

[11] Hasegawa, A., Mima, K. and Duong-van, M., 1985, Plasma distribution function in a superthermal radiation field, Phys. Rev. Lett., Vol.5, 2608

[12] Misra, K. D. and Pandey, R.S., 1995, Generation of whistler emissions by injection of hot electrons in the presence of a perpendicular A.C. electric field, J. Geophys. Res., Vol. 100, 19405

[13] Pandey, R. P., Karim, S.M., Singh, K.M. and Pandey, R.S., 2002, Effect of cold plasma injection on whistler mode instability triggered by perpendicular AC electric field at Uranus, Earth Moon and Planets, Vol. 91, 195

[14] Pandey, R.P., Singh, K.M. and Mishra, N.M., 2008, Cold plasma injection on VLF wave mode for relativistic magnetoplasma with A.C. electric field, Progress In Electromagnetics Research C, Vol. 2, 217

[15] Pandey, R.S., Rajbir Kaur and Srivastava, U.C., 2013, Whistler Mode Wave by Cold Plasma Injection for Relativistic Generalized Loss-Cone Distribution Function in the Magnetosphere of Uranus, International Journal of Advanced Research, Vol. 1, 367

[16] Pandey, R.S., Srivastava, U.C., Pandey, R.P, Prasad, B.B. and Hariom, 2008, Velocity shear ion-cyclotron instability with perpendicular AC electric field, Progress In Electromagnetics Research M, Vol. 3, 177

[17] Pandey, R.S. and Kaur, R., 2012, Generation of low frequency electromagnetic wave by injection of cold electron for relativistic and non-relativistic subtracted bi-maxwellian distribution with perpendicular AC electric field for magnetosphere of Uranus, Progress In Electromagnetics Research B, Vol. 45, 337

[18] Pandey R.S. and Rajbir Kaur, 2014, Study of Whistler Mode Wave by Injection of Relativistic Hot Electrons Beam in the Magnetosphere of Uranus, Progress In Electromagnetics Research M, Vol. 35, 77

## Author' biography with Photo

**R.S. Pandey** received Ph.D. in Applied Physics from Institute of Technology, Banaras Hindu University, India in 1997 and later worked as Research Associate in same department. Currently, he is Head of Department of Physics, Amity Institute of Applied Sciences, Amity University, U.P, India. In 16 years of research experience, he has published over 70 papers in international and national peer-reviewed journals and conferences. He has 2 patents registered and has successfully supervised 2 Ph.D scholars. Presently, he is Principal Invigilator of a project funded by Indian Space Research Organisation (ISRO) and supervisor of 2 Ph.D students. He is also a reviewer for several international journals. His research areas are instabilities in magneto plasma, data analysis, planetary atmosphere, semiconductor plasma, free electron laser etc.

**Rajbir Kaur** obtained M.Sc. in Physics from Department of Physics and Astrophysics, University of Delhi, India in 2010. She is pursuing Ph.D in applied physics from Amity Institute of Applied Sciences, Amity University, India. She has worked as a lecturer in GGS Indraprastha University from 2010 to 2012. She is awarded Senior Research Fellowship from Indian Space Research Organisation (ISRO). She has published about 5 papers in international journals and conferences. Her main research area is magnetospheric plasma and data analysis